Generalised gamma spectrometry simulator for problems in nuclide identification

Turner, Anthony; Wheldon, Carl; Gilbert, Mark; Packer, Lee; Burns, Jon; Kokalova Wheldon, Tzany; Freer, Martin

DOI:
10.1088/1742-6596/1643/1/012211

Generalised gamma spectrometry simulator for problems in nuclide identification

Journal of Physics: Conference Series **1643** (2020) 012211 doi:10.1088/1742-6596/1643/1/012211

Generalised gamma spectrometry simulator for problems in nuclide identification

A. Turner[a], C. Wheldon[a], M.R. Gilbert[b], L.W. Packer[b], J. Burns[c], Tz. Kokalova Wheldon[a], M. Freer[a]

[a] University of Birmingham, Edgbaston, Birmingham, B15 2TT, UK
[b] UKAEA, Culham Science Centre, Abingdon, Oxfordshire, OX14 3DB, UK
[c] AWE plc., Aldermaston, Reading, RG7 4PR, UK

Abstract. Improvements in Radio-Isotope IDentification (RIID) algorithms have always been a continuous research focus. However, significant developments in machine learning have recently sparked renewed interest. To provide a rapid development environment for this, a generalised gamma simulator has been built using the GEANT4 toolkit. This enables consideration of a diverse range of radiation sources and shielding scenarios. The simulator currently provides training data for the development of neural network based RIID models.

1. Introduction

Radio-Isotope IDentification (RIID) algorithms have broad application across alarms and detection, identification, and mapping [1]. Often these are developed in the context of security, but are readily applied to problems in decommissioning and survey [2–6]. The increased accessibility of machine learning techniques has recently produced many exciting new directions for this problem space [7, 8].

Success in these applications come down to the detector, electronics, and the RIID algorithm. Since the widely adopted detectors rarely change, it is the algorithms that often develop. The goal is to infer the identity of all isotopes present in a source and to quantify as many properties as possible [6]. Research is continuous because it can be extremely difficult to automate. There are a myriad of competing effects that can impact gamma ray spectra such as shielding, gain shifts, and changing environmental conditions. Even the system itself is bound by practical considerations of robustness, availability, and affordability [9].

To develop algorithms it has become common practice to use simulated spectra that augment the real data, which are often limited. This requires a simulator that can generate accurate gamma spectra for a diverse range of radiation sources, detectors, and scenarios. Such an environment is conducive to rapid development in RIID.

GEANT4 [10] is chosen to fulfil the role of simulator due an unmatched flexibility when compared with MCNP [11] or GADRAS [12]. Timing information is readily accessible with a GEANT4 based simulator, as are the energy depositions needed to generate a spectrum. The fundamental focus is that of per-decay accuracy rather than a statistical approach, allowing for more subtle effects to be well represented in the resulting spectra.

2. Project scope

A significant part of generalising a simulator is the ability to model multiple detector types. This becomes as simple as swapping out models and redefining a few parameters in the simulator. For these proceedings, evaluations using the HPGe model are chosen for demonstrative purposes. Of course the NaI, $LaBr_3$, and PVT models are also of particular interest to RIID, but many features of the spectrum are clearer with the superior resolution of HPGe.

Bespoke solutions to timing or true coincidence summations are undesirable. MCNP, for example, requires the emission probabilities of every possible particle. Summations must therefore be pre-calculated based on the simulation geometry and detector properties, and be appended to the source definition. This requires additional preprocessing steps liable to user error. True coincidence summations are of particular interest since it is common practice to simulate larger stand-off distances and avoid the issue. By accurately reproducing true coincidence summation peaks, extra information becomes available for RIID algorithms in low activity, close geometry scenarios. Finally, heavily shielded scenarios will be considered as another difficulty RIID typically faces.

3. Producing energy spectra

3.1. Gaussian energy broadening

Fundamental to simulating any gamma-ray spectrum, each energy deposit is sampled from a Gaussian distribution with parameters derived from experimental data. This emulates the expected energy broadening, with the width ($\sigma = fwhm/2\sqrt{\ln(2)}$) from the empirical [13],

$$fwhm = a + b\sqrt{E + cE^2}. \tag{1}$$

Note that this describes full energy peaks that do not involve annihilation photons. In real data, these are broader than expected, leading to a distinctly separate dataset shown in Figure 1. The low energy data have broader FWHM due to contributions from background and other very close transitions, but the empirical fit reproduces the low energy region well when simulated.

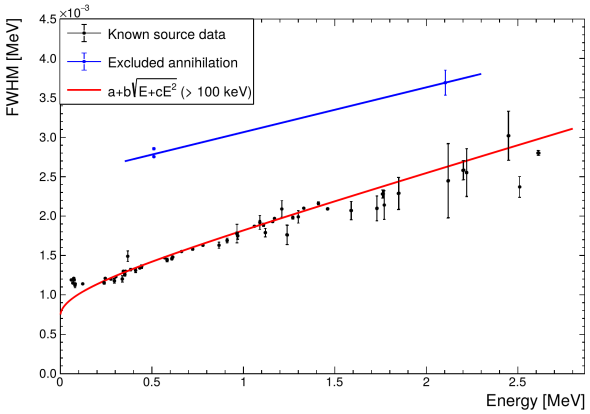

Figure 1. FWHM calibration curve for the HPGe model. Broader annihilation peak related data excluded from core set.

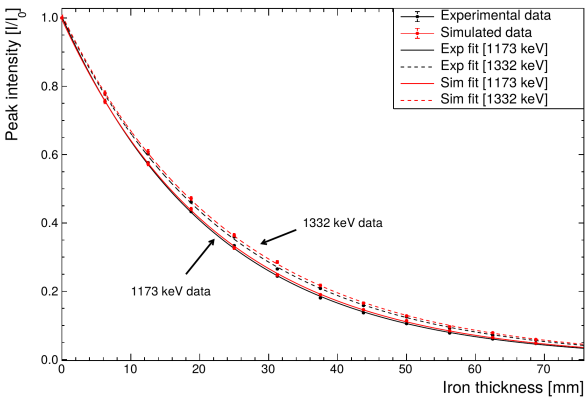

Figure 2. Comparison of gamma attenuation with real data for ^{60}Co, with up to 70 mm of iron plates.

3.2. Annihilation

A net residual momentum of the e^-/β^+ results in additional broadening of these annihilation related events. Below ~2.0 MeV special consideration may be given to the 511 keV. More rigorously, the relevant tracks may be flagged during tracking to force sampling form an alternate parameter set. This may be taken from the annihilation curve shown in Figure 1.

3.3. Decay chain limiting

GEANT4 will follow a decay chain for as long as no stable isotope is reached. This can result in unrealistic spectra over experimental time scales. A perfect example is ^{241}Am alpha decaying to ^{237}Np, which has a 2×10^{6} yr half-life. A cut-off based on lifetime for any secondary nuclei is implemented, killing tracks above an acceptable threshold. Without it, simple spectra like ^{241}Am will end up with contributions from the entire neptunium decay series.

3.4. X-ray fluorescence

While often very minor, the effects of X-ray fluorescence can be represented at the lower energies of gamma spectra. Characteristic X-rays are often emitted following a photoelectric absorption as electrons move to fill the inner-shell vacancy. Since low-energy gamma interactions are more likely to occur close to the crystal surface, these X-rays can escape the crystal without depositing any energy. The resulting feature is known as an X-ray escape peak.

Production cuts are tailored to the detector material. A threshold is set as high as possible while being low enough to allow X-rays to be produced by atomic relaxation models. Only crystal volumes are assigned to a special 'region'. Custom production cuts are specified for these alone, leaving other volumes a compromise between speed and fidelity. This is based on consideration of dead layer attenuation expectations, distance/composition of surrounding materials, and most importantly the impact on the final energy spectrum.

3.5. Multi-isotope sources

The preferred method of simulating a multi-isotope source is to sample from a list of nuclides based on activity, then decay that nuclide for the current event. This is true of most MCNP implementations. Here, all sources are defined at the start of each run, with one nuclide randomly chosen for each event based on relative activity.

For very active sources, where random summations can occur with other sources or even themselves, the probability of two nuclides decaying at the same time for a given mass and activity can be calculated. Sampling based on this probability, multiple nuclides may be defined in the same event and forced to 'decay' at the same time. This is currently unnecessary for RIID purposes. Anything of high enough activity for it to be an issue will be flagged by gross counts alone and can be manually inspected.

3.6. Shielding

Including shielding in the geometry is as simple as modelling it. All elements and their properties are predefined in GEANT4, as are a selection of common materials. New compounds and materials may also be user defined with relative abundances and densities. Taking the simple example of several iron plates between a ^{60}Co source and the detector, the photopeak intensities may be found as a function of thickness (Figure 2). Attenuation coefficients may then be calculated from the exponent.

4. Timing and summation peaks

In GEANT4 every particle propagation object contains a huge amount of information, including tracked times. One of the driving factors for the switch from MCNP to GEANT4 was this access to timing information. Having these times is excellent for setting up multi-detector coincidences, but also crucial for accurate summation peaks. Precise timing and accurate summation peaks are inextricably linked; arrival times are required to decide whether two energy deposits should be summed, and long radioactive time scales make this a challenge to do in a generalised manner.

4.1. Radioactive decay time scales

A 'global time' tracks the time passed since an event began. Its nanosecond base unit is stored in C++ double precision. Rounding inevitably becomes detrimental to timing precision, especially with longer lifetimes. Calculating small time differences after million year half-lives becomes unreliable and will often round to zero. If particles of interest are known it is easy to create bespoke solutions, but for a generalised simulator this must be taken care of automatically.

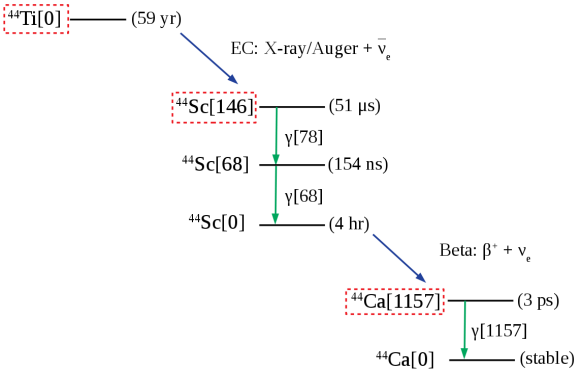

Figure 3. Simplified ^{44}Ti decay scheme.

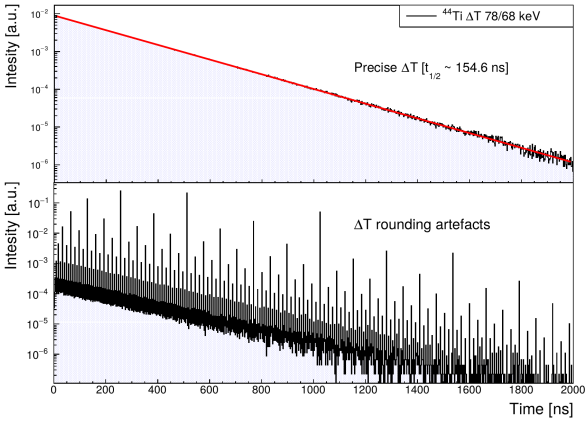

Figure 4. Rounding artefacts in timing.

Taking the ^{44}Ti decay chain as an example (Figure 3), the difference in creation times of the 68 keV and 78 keV photons are collected. Experimentally this investigates the half-life of the interim ^{44}Sc excited state. Simply subtracting global times results in the artefacts seen in Figure 4, even after a relatively short 59 yr initial half-life.

Resetting the global time to zero at key points is the simplest solution, noting when a reset happens. Time differences are then calculated relative to the nearest common reset point rather than the start of an event. In doing so, magnitudes are kept small enough that rounding is no longer an issue.

For example, a reset point at ^{44}Sc[146] (shown in Figure 3) can be forced. The global times being subtracted for the previous calculation are now on the order of microseconds rather than years. By implementing code to check time differences between any two given secondary particles, a 'trigger' system analogous to experimental methods can be set up based on energy. With global time magnitudes now under control, the same subtraction produces an exponential without rounding errors, as seen in the top half of Figure 4. This works well for even a 17 ps state in ^{208}Tl after the full ^{232}Th decay chain (in which it is populated) is followed within a single event.

4.2. True coincidence summing

Following a radioactive decay in GEANT4, the entire series of secondary photons and particles becomes part of the same event. True summations therefore naturally occur in these simulations. Taking ^{60}Co as a standard example, the intensities of two primary photo-peaks and their corresponding sum peak may be compared to experimental data (Figure 5).

The trends closely follow a solid angle (Ω) dependence as expected, becoming Ω^2 for the summation. A naïve approach to energy deposition, where everything entering the crystal is summed, works fine for ^{60}Co. However, for more complex decay schemes it can result in spurious summations (Figure 6). Any ^{44}Sc emissions occur *hours* before any annihilation photons in the ^{44}Ti example of Figure 3.

To solve this, time differences between tracks in the crystal must be found and handled accordingly. For gamma detectors all energy deposition comes from secondary particles produced

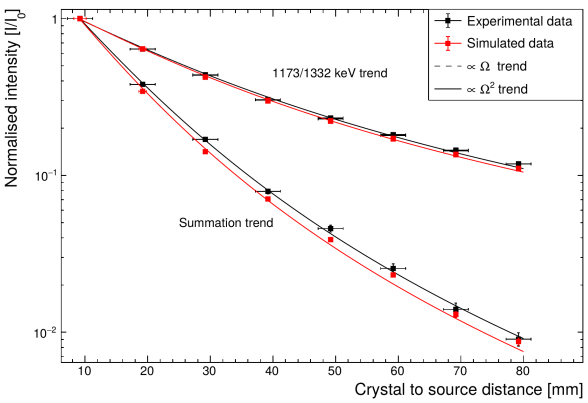

Figure 5. ^{60}Co photo-peak intensities as a function of source distance.

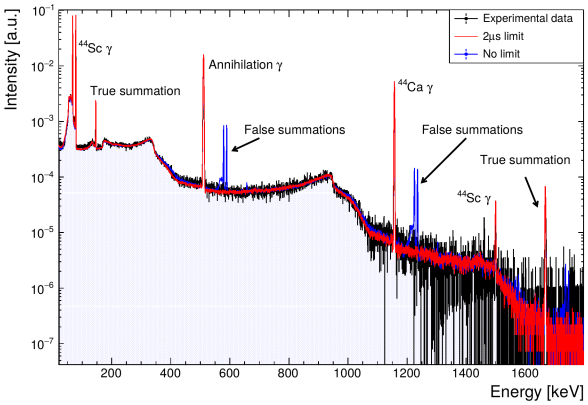

Figure 6. Demonstration of spurious ^{44}Ti summations with no timing information used.

within the crystal. Reconstruction of full, independent tracks is therefore carried out by following parent-child chains. Once reconstructed, the total energy deposited for each track may either be summed or considered separate based on an appropriate time window.

A 2 μs window for the ADC conversion time seen in the red spectrum of Figure 6 demonstrates this method removing spurious peaks while keeping accurate true summations. This generalised use for any source is only possible by maintaining good timing precision over radioactive decay time scales.

4.3. Multi-detector coincidences

With precision maintained in emission time differences, only travel times are further required to allow for multi-detector coincidence measurements. Summation peaks also simply need an extra condition to check that two candidate tracks enter the same detector.

A coincidence measurement is a combination of emission and travel time differences, with broadening from intrinsic physical properties like scintillation lifetimes. Just as energy resolution is sampled from a Gaussian based on experimental data, so too is a time resolution. Figure 7 shows the inclusion of an arbitrary 35 ns time resolution. The fit in this figure is a convolution of a Gaussian and exponential [14], confirming accurate representation of the simulation parameters.

With multiple detectors and good timing information, angular correlations may also be investigated. At the time of writing, the GEANT4 source only has a demonstrative implementation for select isotopes; the simple $4^+ \rightarrow 2^+ \rightarrow 0^+$ cascade in ^{60}Co. Checking with ^{108m}Ag it is clear that any angular correlations must be manually implemented by the user.

Of course, the $4^+ \rightarrow 2^+ \rightarrow 0^+$ cascade in ^{108m}Ag mirrors that of ^{60}Co and works well (Figure 8). However, no correlation is seen for the $6^+ \rightarrow 4^+ \rightarrow 2^+$ cascade in the same decay. While the amplitude should be slightly suppressed, the phase should be exactly the same as the transitions that follow.

5. Current limitations

As with any simulator there are inherent limitations in fidelity achievable due to environmental effects. The Naturally Occurring Radioactive Background (NORM) is primarily from the ^{235}U and ^{232}Th decay series, along with a significant ^{40}K photopeak. This corresponds to contributions from only ∼25 distinct radioactive nuclides. However, local contaminations, activations, and relative intensities all make it difficult to define a representative template. The same is true of backscatter contributions to spectra. Any photons scattering back into the detector from surrounding materials are dependent on accurate reproduction of the nearby environment.

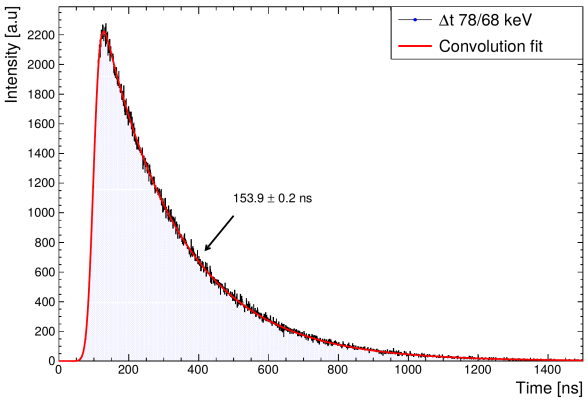

Figure 7. Example time spectrum for half-life measurement of ^{44}Sc.

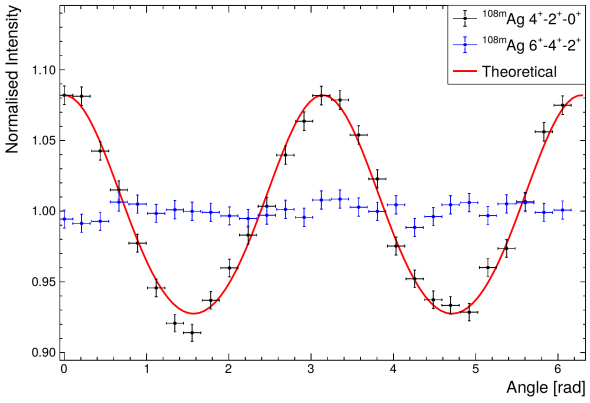

Figure 8. Demonstration of limited angular correlation implementation using ^{108m}Ag.

6. Simulator usage

This simulator is currently serving the crucial role of providing machine learning models with training data. These data are generated as needed for rapid testing of diverse scenarios. Of course, corresponding test data are experimentally collected for final evaluations to present better representations of real world performance. Accurate coincidence summations allow investigations of closer geometries, and whether the additional peaks are useful for improved RIID. Setting up multiple detectors also provides coincidence data that may give the machine learning models extra relevant information.

References

[1] C.J. Sullivan and J. Lu. Automated photopeak detection and analysis in low resolution gamma-ray spectra for isotope identification. *Nuclear Science Symposium and Medical Imaging Conference*, IEEE, 2013. DOI: 10.1109/NSSMIC.2013.6829437.

[2] J.M. Blackadar. Automatic isotope identifiers and their features. *IEEE Sensors Journal*, 5(4):589–592, 2005. DOI: 10.1109/JSEN.2005.846374.

[3] T. Burr, M.S. Hamada, T.L. Graves, and S. Myers. Augmenting real data with synthetic data: an application in assessing Radio-Isotope identification algorithms. *Quality and Reliability Engineering International*, 25(8):899–911, 2009. DOI: 10.1002/qre.1003.

[4] C.J. Sullivan, S.E. Garner, M. Lombardi, K.B. Butterfield, and M.A. Smith-Nelson. Evaluation of key detector parameters for isotope identification. *IEEE Nuclear Science Symposium Conference Record*, 2:1181–1184, 2007. DOI: 10.1109/NSSMIC.2007.4437217.

[5] D.C. Stromswold, J.W. Darkoch, J.H. Ely, R.R. Hansen, R.T. Kouzes, B.D. Milbrath, R.C. Runkle, W.A. Sliger, J.E. Smart, D.L. Stephens, L.C. Todd, and M.L. Woodring. Field tests of a NaI(Tl)-based vehicle portal monitor at border crossings. *Nuclear Science Symposium Conference Record*, IEEE, 2004. DOI: 10.1109/NSSMIC.2004.1462180.

[6] T. Burr and M. Hamada. Radio-Isotope Identification Algorithms for NaI γ Spectra. *Algorithms*, 2(1):339–360, 2009. DOI: 10.3390/a2010339.

[7] M. Kamuda, J. Stinnett, and C.J. Sullivan. Automated Isotope Identification Algorithm Using Artificial Neural Networks. *IEEE Transactions on Nuclear Science*, 64(7):1858–1864, 2017. DOI: 10.1109/TNS.2017.2693152.

[8] D. Liang, P. Gong, X. Tang, P. Wang, L. Gao, Z. Wang, and R. Zhang. Rapid nuclide identification algorithm based on convolutional neural network. *Seminars in nuclear medicine*, 133:483–490, 2019. DOI: 10.1016/j.anucene.2019.05.051.

[9] M. Swoboda, R. Arlt, V. Gostilo, A. Lupilov, M. Majorov, M. Moszynski, and A. Syntfeld. Spectral gamma detectors for hand-held radioisotope identification devices (RIDs) for nuclear security applications. *IEEE Transactions on Nuclear Science*, 52(6):3111–3118, 2005. DOI: 10.1109/NSSMIC.2004.1466839.

[10] S. Agostinelli et al. Geant4 - a simulation toolkit. *Nuclear Instruments and Methods in Physics Research Section A*, 506(3):250–303, 2003. DOI: 10.1016/S0168-9002(03)01368-8.

[11] T. Goorley et al. Initial MCNP6 Release Overview. *Nuclear Technology*, 180(3):298–315, 2012. DOI: 10.13182/NT11-135.

[12] S.M. Horne, G.G. Thoreson, L.A. Theisen, D.J. Mitchell, L. Harding, and W.A. Amai. GADRAS-DRF 18.5 User's Manual. *Sandia National Lab, Technical Report*, 2014. DOI: 10.2172/1166695.

[13] G. Gilmore. *Practical Gamma-ray Spectroscopy, 2nd Edition*. John Wiley and Sons, 2011. ISBN 9781119964698.

[14] C. Wheldon. *Convolution of a Gaussian with an exponential (and its application in programs halflife.c/nanofit.f)*. University of Birmingham, 2014.